

Comparison of Two Biosorbent Beads for Methylene Blue Discoloration in Water

Gani Purwiandono^{1*}, Puji Lestari²

¹ Department of Chemistry, Faculty of Mathematics and Natural Sciences, Universitas Islam Indonesia, Jl. Kaliurang Km. 14.5, Yogyakarta 55584, Indonesia

² Department of Environmental Engineering, Faculty of Civil Engineering and Planning, Universitas Islam Indonesia, Jl. Kaliurang Km. 14.5, Yogyakarta 55584, Indonesia

* Corresponding author's e-mail: gani_purwiandono@uii.ac.id

ABSTRACT

In this study, alginate-encapsulated biosorbents have been prepared from agricultural wastes viz. peanut shells and rice husks. Biosorbents in this study were referred as En-PS and En-RH for the adsorbents prepared from peanut shells and rice husks, respectively. The characteristics of the adsorbents were thoroughly investigated using scanning electron microscope, X-ray diffractometer, surface area analyzer, and Fourier-transform infrared spectrophotometer instruments. The prepared biosorbents were used as adsorbents for cationic methylene blue (MB) dye in water. The encapsulation process using sodium alginate simplified the separation of adsorbent from the water after the adsorption process. The adsorptions of MB onto both adsorbents followed the pseudo-second order model and fitted both Langmuir and Freundlich isotherm models. Thermodynamic studies revealed that the adsorption of MB onto En-PS and En-RH was a spontaneous and endothermic process with the ΔG° reaction of -1.694 and -2.028 kJ/mol at the room temperature, respectively. Biosorbents could be used in the adsorption-desorption process for up to 3 cycles.

Keywords: adsorption, alginate-encapsulated, biosorbents, methylene blue.

INTRODUCTION

Synthetic dyes have been widely applied in various industries, including textile, pharmaceutical, paper, dye, plastic, etc. The presence of dyes in industrial effluent, may cause aesthetic and environmental problems even in a low concentration. Synthetic dyes are resistant to photo-oxidation and biodegradation processes in nature (Garg et al., 2019). The colored water reduces the sunlight penetration into water bodies, thus reducing the photosynthesis of aquatic plants. Synthetic dyes are carcinogenic, mutagenic, and toxic for humans (Al-Tohamy et al., 2022). Hence, the removal of synthetic dyes from wastewater is highly necessary.

Many technologies have been developed to remove dyes from dye-containing wastewater, such as chemical precipitation (Alotaibi et al.,

2019), ion exchange (Khan et al., 2022), membrane filtration (Marszałek and Żyła, 2021), oxidation process (Abdel-Aziz et al., 2018), adsorption (Rashid et al., 2021), bio removal (Vishnu et al., 2022), etc. Among those technologies, adsorption is the most effective technique due to the simple operation and design, ability to remove pollutants, low-cost process and the possibility of reuse and regeneration of the used adsorbent (Costa et al., 2022).

Compared to the chemical and electrochemical processes, such as oxidation process, electrocoagulation, and bio removal; the physicochemical processes, such as chemical precipitation, ion exchange, membrane filtration, and adsorption were more efficient and required lower energy consumption (Peng and Guo, 2020). Biosorbents are adsorbent materials developed from natural materials and agricultural wastes that are rich in

certain functional groups such as carboxyl and hydroxyl groups, which have a high affinity for pollutants in aqueous solution. Biosorbents obtained from agricultural waste are promising materials due to their availability, renewable properties, and low production cost (Lucaci et al., 2020). The use of agricultural waste-derived biosorbents will add the value of the agricultural wastes and reduce the cost needed for their disposal. Those benefits essentially motivate the extensive usage of biosorbent in experimental studies (Orooji et al., 2022).

Peanut shells and rice husks are two examples of agricultural wastes that can be used as a low-cost biosorbent for dyes in water. Peanut shells contain high cellulose, hemicellulose, and lignin (Khiaophong et al., 2022; Sah et al., 2022). Some studies have reported the ability of activated carbon derived from peanut shells to remove aqueous pollutants, including dye. Rice husks have also been reported to be able to be used as adsorbents for pollutants in water (Saghir et al., 2022; Yu et al., 2016; Khaniabadi et al., 2017).

Bare biosorbents prepared from agricultural waste are mainly in the form of fine powder that limits the adsorption process because the separation of the powdery adsorbents from water requires further separation processes such as centrifugation or filtration. To overcome this disadvantage, the encapsulation of the fine powders is an alternative solution. The encapsulation process could immobilize the fine adsorbent powder and change the fine powders into granules and further simplify the separation of adsorbents after the adsorption process.

This study aims to synthesize biosorbents based on rice husks and peanut shells and encapsulate them with sodium alginate. The comparison of the encapsulated rice-husk (En-RH) and the encapsulated peanut shells (En-PS) biosorbents for methylene blue (MB) adsorption from water was studied for the first time. This study offers a framework for examining the use of environmentally benign agricultural waste material as an effective and efficient biosorbents for synthetic dye in water.

METHODS

Materials

Peanuts were collected from the local market in Yogyakarta, Indonesia and peeled to obtain the shells. Rice husks were obtained from the local rice field in Yogyakarta, Indonesia. Peanut shells

and rice husks were utilized as the raw materials for biosorbent synthesis. Sodium alginate (Sigma Aldrich), 0.5 M calcium chloride (93%, Merck), 0.1 M hydrochloric acid (37%, Merck), nitric acid (91%, Merck), and MB dye (Merck) were of analytical grade and were directly used as received from the manufacturers. Distilled water was used to prepare the solution.

Preparation and characterization of alginate encapsulated peanut shell (En-PS) and alginate encapsulated rice husks (En-RH) adsorbents

Peanut shells were thoroughly and repeatedly washed with water to remove dirt and impurities and then dried at 105 °C to constant weight. Rice husks were separated from the leaves and the rice straw and dried at 105 °C to remove water. Dried peanut shells and rice husks were ground and sieved with a 150-mesh sieve. Peanut shell and rice husk powders were activated by soaking in dilute HNO₃ for 6 h. After soaking, the materials were filtered, washed to neutral and dried in the oven at 105 °C.

Sodium alginate hydrogel was prepared for the encapsulation process by dissolving 1 g of sodium alginate powder in 50 mL water (two series of solutions). The solutions were stirred until sodium alginate was completely dissolved and the hydrogel was formed. As much as 2.5 g of peanut shell and rice husk powders were added to each hydrogel. The mixture was then sonicated for 45 min at room temperature. The mixture was poured into 0.5 M CaCl₂ solution drop wisely to form the En-PS (encapsulated peanut shell) and En-RH (encapsulated rice husk) beads. The beads were washed repeatedly with water to remove the calcium ion and oven-dried at 105 °C to constant weight.

The surface morphologies of En-PS and En-RH were characterized using Scanning Electron Microscope (SEM, Hitachi S-4800, Japan) instrument. X-ray diffraction (XRD, Rigaku Ultima II, Japan) of the adsorbents was performed using X-ray diffractometer instrument with CuK radiation. The presence of functional groups on the adsorbent materials were investigated using Fourier Transform Infrared Spectrophotometer (Perkin Elmer, spectrum II, America), the surface area analyzer (SAA, Quantachrome Novatouch Lx4) was used to investigate the surface area of the materials.

Adsorption experiments

MB solutions were prepared from MB stock solution and the solution pH was adjusted using dilute HCl and NaOH. The adsorption experiment was conducted in a closed batch system by interacting an amount of each adsorbent with MB solution. After the adsorption reached equilibrium, the used adsorbent was separated, and the MB concentration that remained in the solution was measured using UV-Visible spectrophotometer (Hitachi, U-4100 Spectrophotometer) with λ_{max} of 663 nm. Effect of parameters including pH, contact time, initial concentration of MB, adsorbent mass, and temperature were investigated. The removal efficiency (%) of adsorption process was calculated using Eq. 1.

$$\text{Removal efficiency (\%)} = \frac{(C_0 - C_e)}{C_0} \times 100 \quad (1)$$

where: C_0 – the initial concentration of MB ($\text{mg} \cdot \text{L}^{-1}$); C_e – the concentration of MB after adsorption process ($\text{mg} \cdot \text{L}^{-1}$). The experimental adsorption data was obtained from the average values of triplicates. The reusability of adsorbents was studied using 3 adsorption-desorption process cycles.

RESULTS AND DISCUSSION

Characterization of adsorbents

Peanut shells and rice husks, like other agricultural biomasses, contain high amount of lignin, cellulose, and hemicellulose. FTIR spectra of En-RH and En-PS are given in Figure 1a. The broad band at around 3350 cm^{-1} for En-RH and En-PS is assigned to the hydroxyl group (OH) of alcoholic, phenolic, and carboxylic derivatives. The absorption peak at 2920 cm^{-1} is the absorption band of C-H asymmetrical stretching of aromatics, aliphatic and olefins in lignin structure (Saghir et al., 2022). The absorption bands between 1734 and 1605 cm^{-1} are assigned to C=O groups in carbonyl, ketones, and aldehydes and to C=C present in the aromatic rings. A sharp absorption peak further confirms the presence of aromatic rings at 1030 cm^{-1} . En-PS and En-RH show relatively similar FTIR spectra, indicating that the functional groups in both adsorbents are similar. X-ray diffractogram of En-PS and En-RH in Figure 1b showed the semi-crystalline nature of sodium alginate that encapsulated the peanut shells and rice husks powders. Surface morphologies of En-PS and En-RH in Figure 1(c, d) showed relatively smooth surface of both En-PS and En-RH.

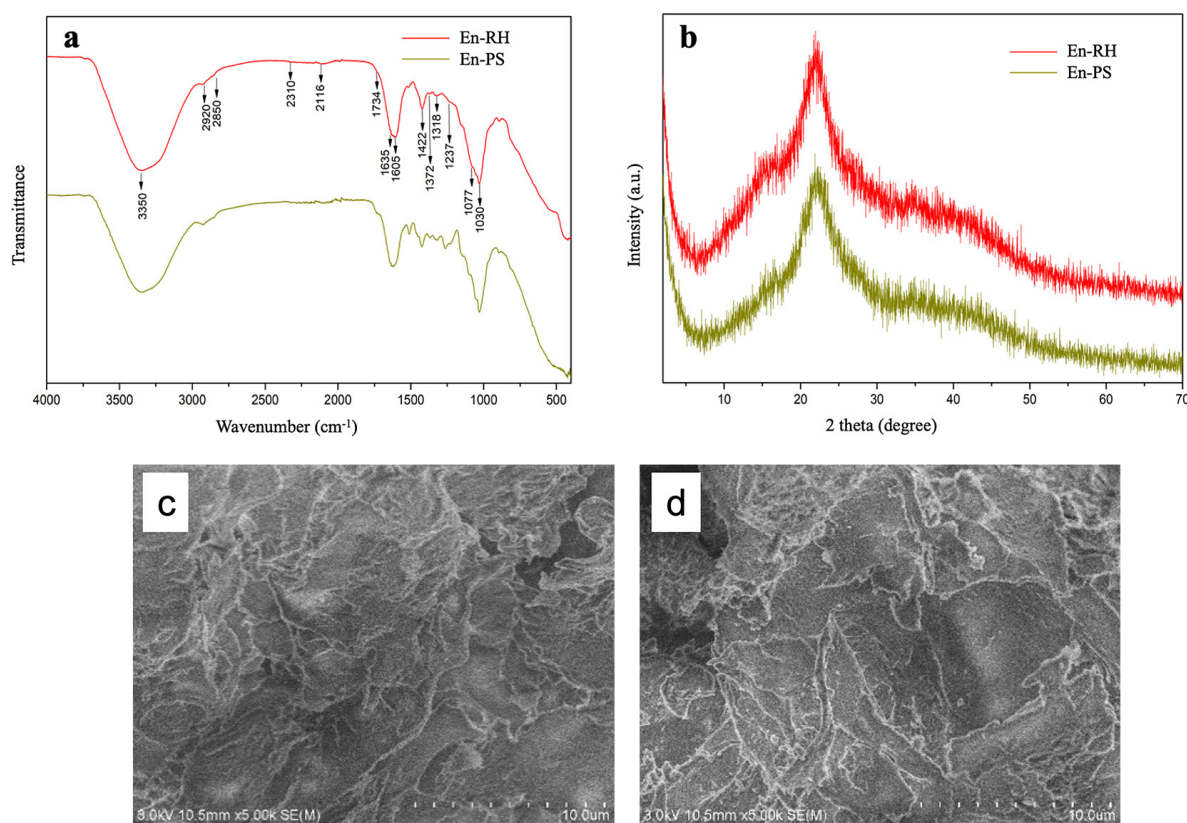


Figure 1. FTIR spectra (a), XRD diffractogram (b) of the adsorbents, SEM images of En-PS (c), and En-RH (d)

Adsorption studies

In the adsorption process, pH is crucial in determining the functional groups of both adsorbent and adsorbate. In this study, the effect of pH on adsorption of MB onto En-RH and En-PS was studied at pH range from 3 to 11 and the result is presented in Figure 2a. The adsorption of MB onto En-RH and En-PS showed a similar trend with removal efficiency of En-RH being higher than that of En-PS. The higher removal efficiency of MB using En-RH is likely due to the higher total pore volume of En-RH (Figure 2d). It is seen that the efficiency of the adsorption increases with the increase of solution pH. At low pH values, the adsorbent is positively charged which resulted in the decrease of adsorption of cationic MB. At higher pH, the OH-containing functional groups of the adsorbents will deprotonate to form negatively charged functional groups, which causes the optimum interaction with the positively charged MB dye cation. The pKa value of MB dye is 3.8, thus, at pH higher than 3.8 the cationic species of MB dye is predominant in the solution.

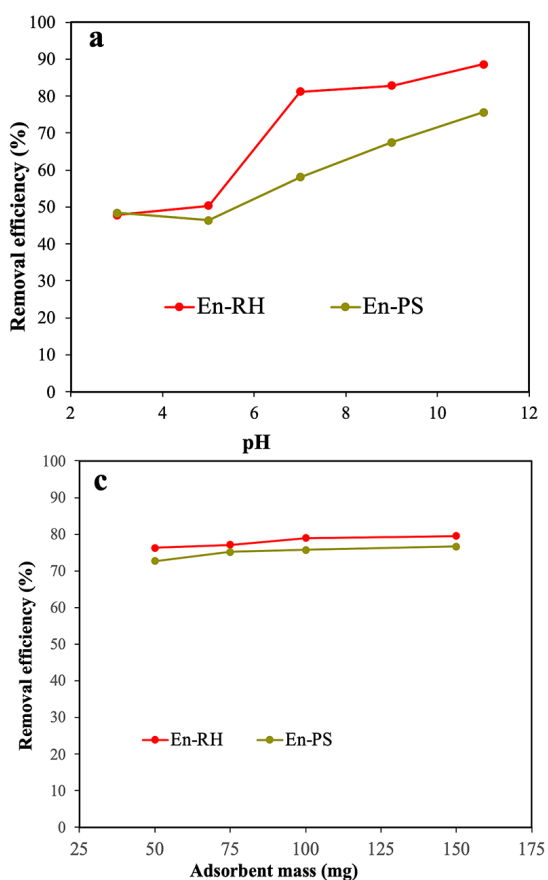


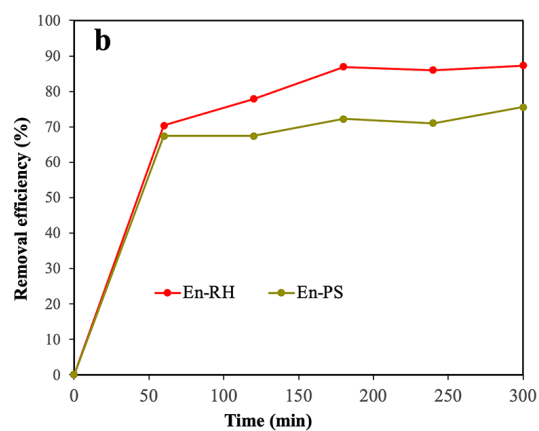
Figure 2. pH versus removal efficiency of MB (a), contact time versus removal efficiency of MB (b), adsorbent mass versus removal efficiency of MB (c), the porosity of En-RH and En-PS (d)

Figure 2b shows that at the initial stage of the adsorption, both En-PS and En-RH showed a sharp increase (70% for En-RH and 67% for En-PS) in MB adsorption due to the high availability of the active sites on the surface of the adsorbents. With the increase of interaction time, the adsorption of MB gradually increases until equilibrium is reached at 180 min. After 180 min, the removal efficiency of MB increases insignificantly or relatively constant.

Figure 2c showed the adsorption of MB using various dosages of both adsorbents. The adsorbent mass above 50 mg had no effect on the adsorption efficiency of MB onto both En-PS and En-RH from solution. In this investigation, there is no association between adsorbent mass and adsorption efficiency. It is also worth noticing that both biosorbents En-PS and En-PS have a potential application for dye degradation.

Adsorption kinetics

The adsorption kinetics was studied to understand the adsorption mechanism as well as to



d

Adsorbent	Specific pore (m ² g ⁻¹)	Total pore volume (cm ³ g ⁻¹)
En-RH	29.60	0.071
En-PS	18.80	0.034

evaluate the efficiency of the adsorbent. The adsorption kinetics was studied using pseudo-first order and pseudo-second order kinetic models. The equations of pseudo-first order and pseudo-second order kinetic model are given by Eq. 2 and 3, respectively.

$$\ln(q_e - q_t) = -k_1 t + \ln q_e \quad (2)$$

$$\frac{t}{q_t} = \frac{1}{k_2 q_e^2} + \frac{t}{q_e} \quad (3)$$

Parameter q_e is the amount of MB adsorbed on the adsorbents at equilibrium (mg g^{-1}), q_t (mg g^{-1}) is the amount of MB adsorbed on the adsorbents at time t (min), k_1 is the adsorption rate constant of pseudo-first order kinetic model (min^{-1}) and k_2 is the adsorption rate constant of pseudo-second order kinetic model ($\text{g mg}^{-1} \text{min}^{-1}$).

A typical plot of pseudo-second order kinetics model is presented in Figure 3. The high linearity of the graph showed that the adsorption of MB

onto both En-PS and En-RH followed the pseudo-second order kinetic model. The adsorption kinetic parameters of the adsorption processes are summarized in Table 1. Pseudo-second order kinetic model assumes that the rate-limiting step is chemical sorption, and the rate of adsorption depends on the adsorption capacity, not on concentration of the adsorbate (Sawalha et al., 2022; Turan and Turan, 2022). Table 1 showed the kinetic parameters of MB adsorption on both biosorbents.

Adsorption isotherms

The adsorption isotherm models were evaluated to reveal the interaction mechanism of MB dye with the active sites of the adsorbent. Langmuir and Freundlich isotherm models were used in this study. The linear equations of Langmuir and Freundlich isotherm models are given in Eq. 4 and 5, respectively.

$$\frac{1}{q_e} = \frac{1}{q_m} + \frac{1}{K_L q_m C_e} \quad (4)$$

$$\log q_e = \log K_F + \frac{1}{n} \log C_e \quad (5)$$

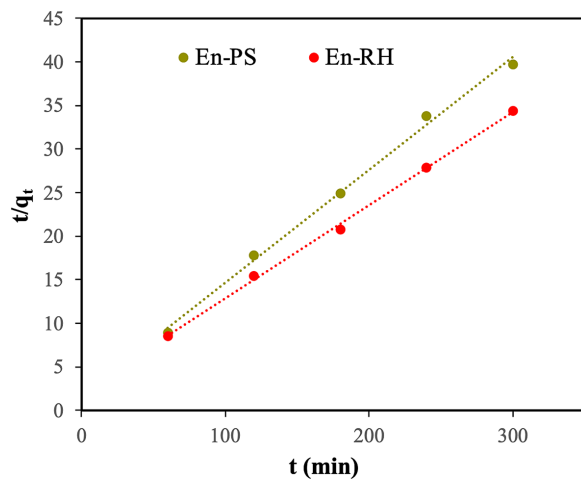


Figure 3. Plot t versus t/q_t

Table 1. Kinetics parameters MB adsorption

Adsorption kinetic parameters	En-PS	En-RH
Pseudo-first order model		
q_e (mg g^{-1})	1.10	4.66
k_1 (min^{-1})	0.0045	0.0183
R^2	0.592	0.660
Pseudo-second order		
q_e (mg g^{-1})	7.73	9.35
k_2 ($\text{g mg}^{-1} \text{min}^{-1}$)	0.0095	0.0053
R^2	0.996	0.998

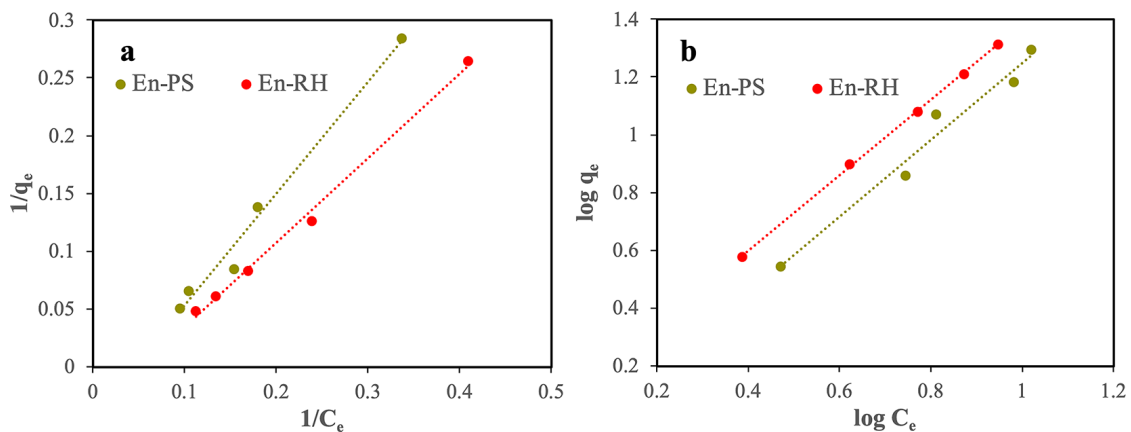


Figure 4. Plot $1/C_e$ versus $1/q_e$ (a); plot $\log C_e$ versus $\log q_e$ (b)

where: q_e – the amount of MB adsorbed on the adsorbent at equilibrium (mg g^{-1});
 q_m – the Langmuir maximum adsorption capacity (mg g^{-1});
 C_e – the concentration of MB in solution at equilibrium (mg L^{-1});
 K_L – the Langmuir constant;
 K_F and n – Freundlich adsorption constants.

The adsorption of MB dye onto En-PS and En-RH fitted well both Langmuir and Freundlich isotherm models, as shown in Figure 4. It means that both models are suitable for describing the adsorption mechanism of MB onto both biosorbents.

All isotherm parameters of the adsorption processes in this study are summarized in Table 2. Maximum adsorption capacity (q_{max}) of En-RH and En-PS for MB dye is comparable with other biosorbents reported in previous studies as summarized in Table 3. Furthermore, biosorbents beads in this study can be separated easily from the solution after the adsorption process.

Adsorption thermodynamics

Thermodynamic studies were conducted to check the spontaneity and feasibility of the adsorption process, since the calculated thermodynamic parameters such as heat of enthalpy (ΔH°), Gibbs free energy (ΔG°), and entropy (ΔS°) govern the feasibility and spontaneity of the adsorption process, ΔH° , ΔG° , and ΔS° were calculated using Eq. 6–8.

$$\Delta G^\circ = RT \ln K_D \tag{6}$$

$$\Delta G^\circ = \Delta H^\circ - T \Delta S^\circ \tag{7}$$

$$\ln K_D = \frac{-\Delta H^\circ}{RT} + \frac{\Delta S^\circ}{R} \tag{8}$$

where: K_D – the distribution coefficient that was obtained from the amount of MB adsorbed on the adsorbent at equilibrium (q_e) divided by the concentration of MB at equilibrium (C_e).

Figure 5 showed that the adsorption of MB onto En-PS and En-RH were more favorable at higher temperatures, and the adsorption efficiency reduced at lower temperatures. The negative value of ΔG° indicated that the adsorption processes are feasible and spontaneous in nature (Al-Kadhi, 2019; Kali et al., 2022; Khatami et al., 2019). The positive values of enthalpy indicated that the adsorption of MB onto En-PS and EN-RH is an endothermic process. The positive values of entropy suggested that the adsorption of MB on both adsorbents was accompanied by the increase in randomness at the solid/solution interface during the adsorption process (Gökırmak Söğüt, 2022; Teshager et al., 2022; Sarojini et al., 2022). ΔH° value of adsorption of MB on En-RH and En-PS, indicating that both the adsorption reaction could occur in an endothermic condition. The negativity of ΔG° increases with the temperature increase, and this negative value increases rapidly in chemical adsorption (En-PS) than in physical adsorption (En-RH). All thermodynamic parameters are summarized in Table 4.

Table 2. Adsorption isotherm parameters of MB dye adsorption

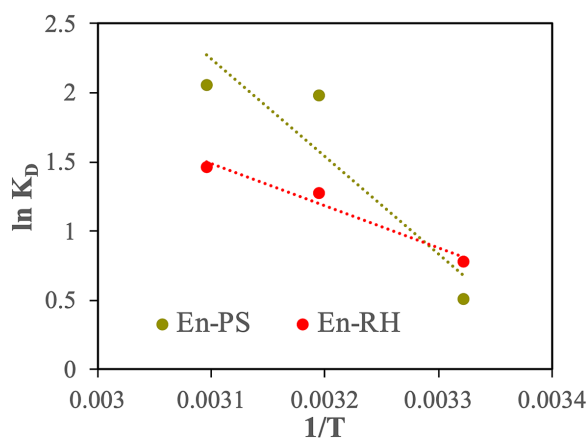
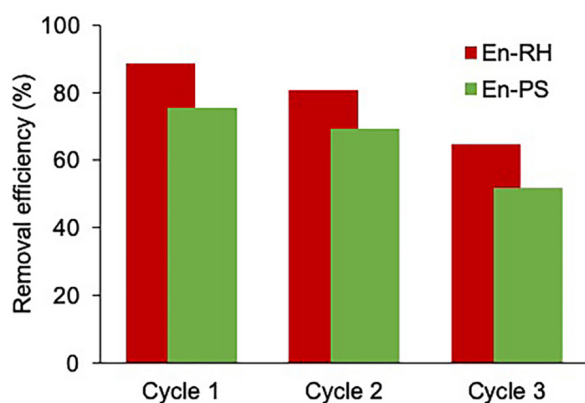
Adsorbents	Langmuir isotherm			Freundlich isotherm		
	q_{max} (mg g^{-1})	K_L	R^2	n	K_F	R^2
En-PS	22.8	1.034	0.984	0.750	0.823	0.972
En-RH	25.9	1.370	0.995	0.767	1.194	0.999

Table 3. Maximum adsorption capacity of some biosorbents for MB dye

Biosorbents	Maximum adsorption capacity, q_{max} (mg g^{-1})	References
Walnut shell powder	36.632	Uddin and Nasar, 2020
Natural rice husk	19.77	Adelodun et al., 2020
Modified wheat husk	4.23	Banerjee et al., 2014
Cashew nutshell	5.31	Senthil Kumar et al., 2011
Yellow passion fruit	44.70	Pavan et al., 2008
Alginate-encapsulated rice husk (En-RH)	25.9	This study
Alginate-encapsulated peanut shell (En-PS)	22.8	This study

Table 4. Thermodynamic parameters of MB dye adsorption

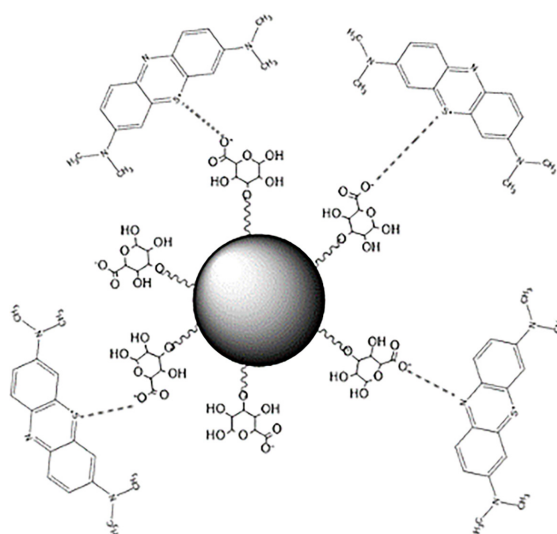
Adsorbent	ΔH (J mol ⁻¹)	ΔS (J mol ⁻¹ K ⁻¹)	ΔG (kJ mol ⁻¹)		
			301 K	313 K	323 K
En-PS	58.636	0.200	-1.694	-4.100	-6.104
En-RH	25.274	0.091	-2.028	-3.116	-4.023

**Figure 5.** Plot $1/T$ versus $\ln K_D$ **Figure 6.** The reusability of En-RH and En-PS on the removal efficiency of MB

The stability and reusability of the biosorbent is some of the critical factors in assessing the potential for commercial applications (Sahmoune, 2019). The stability and reusability of En-PS and En-RH biosorbents for methylene blue adsorption were presented in Figure 6. The removal efficiency of methylene blue adsorption-desorption in 3 consecutive adsorption-desorption cycles showed that the biosorbents could be used repeatedly in the adsorption process. A plausible schematic diagram of adsorption the mechanism of MB adsorption by En-RH and En-PS beads is depicted in Figure 7. The alginate molecule covering the En-RH and En-PS biosorbents provides the -O- groups which can attach MB molecules to the biosorbents through the interaction between -O- from alginate and -N and -OH from MB.

CONCLUSIONS

In this study, alginate-encapsulated biosorbents based on peanut shells and rice husks, En-PS and En-RH, were prepared as adsorbents for methylene blue (MB) dye from water. Adsorbents En-PS and En-RH have similar characteristics in terms of surface morphology, crystallinity, and functional groups. MB adsorptions on En-PS and

**Figure 7.** A plausible schematic diagram of adsorption the mechanism of MB adsorption by En-RH and En-PS beads

En-RH followed pseudo-second order kinetic model with the adsorption rate constant (k_2) of En-PS being higher than that of En-RH. Adsorption isotherms fitted Langmuir and Freundlich isotherm models. Thermodynamic parameters in this study suggested that MB adsorption on both adsorbents was endothermic in nature, feasible and spontaneous. The alginate encapsulation of adsorbent beads reduced the need to separate old adsorbents from water by filtering or centrifugation. Thermodynamic investigations demonstrated that the adsorption of MB onto En-PS and En-RH was spontaneous and endothermic at room temperature, with ΔG values of -1.69 and -2.02 kJ/mol, respectively.

Acknowledgements

This research is funded by *Direktorat Penelitian dan Pengabdian Masyarakat (DPPM)* of Universitas Islam Indonesia under the grant number 001/Dir/DPPM/70/Pen.Pemula/XI/2021.

REFERENCES

1. Abdel-Aziz, M.H., Bassyouni, M., Zoromba, M.S., Alshehri, A.A. 2018. Removal of dyes from waste solutions by anodic oxidation on an array of horizontal graphite rods anodes. *Ind. Eng. Chem. Res.*, 58(2), 1004–1018. <https://doi.org/10.1021/acs.iecr.8b05291>
2. Adelodun, B., Ajibade, F., Abdulkadir, T., Bakare, H., Choi, K. 2020. SWOT analysis of agro-waste based adsorbents for persistent dye pollutants removal from wastewaters. *Environ. Degrad. Causes Remediat. Strateg.*, 88–103. <https://doi.org/10.26832/aesa-2020-edcrs-07>
3. Alotaibi, N.F., Nassar, A.M., Alrwaili, G.M., Elnasr, T.A.S., Abo Zeid E.F. 2019. Selective, efficient and complete precipitation of anionic dyes in aqueous solutions using Ag@PbCO₃ nanocomposite. *Inorg. Nano-Metal Chem.*, 49, 395–400. <https://doi.org/10.1080/24701556.2019.1661463>
4. Al-Kadhi, N.S. 2019. The kinetic and thermodynamic study of the adsorption Lissamine Green B dye by micro-particle of wild plants from aqueous solution. *Egypt. J. Aquat. Res.*, 45, 231–238. <https://doi.org/10.1016/j.ejar.2019.05.004>
5. Al-Tohamy, R., Ali, S.S., Li, F., Okasha, K.M., Mahmoud, Y.A.-G., Elsamahy, T., Jiao, H., Fu, Y., Sun, J. 2022. A critical review on the treatment of dye-containing wastewater: Ecotoxicological and health concerns of textile dyes and possible remediation approaches for environmental safety. *Ecotoxicol. Environ. Saf.*, 231, 113160. <https://doi.org/10.1016/j.ecoenv.2021.113160>
6. Banerjee, S., Chattopadhyaya, M.C., Uma, Sharma, Y.C. 2014. Adsorption Characteristics of Modified Wheat Husk for the Removal of a Toxic Dye, Methylene Blue, from Aqueous Solutions. *J. Hazard. Toxic Radioact. Waste*, 18, 56–63. [https://doi.org/10.1061/\(ASCE\)HZ.2153-5515.0000191](https://doi.org/10.1061/(ASCE)HZ.2153-5515.0000191)
7. Costa, T.C., Hendges, L.T., Temochko, B., Mazur, L.P., Marinho, B.A., Weschenfelder, S.E., Florido, P.L., Silva, A., Souza, A.A.U., Souza, M.A.G.U. 2022. Evaluation of the technical and environmental feasibility of adsorption process to remove water soluble organics from produced water: A review. *J. Pet. Sci. Eng.*, 208, 109360. <https://doi.org/10.1016/j.petrol.2021.109360>
8. Garg, D., Majumder, C.B., Kumar, S., Sarkar, B. 2019. Removal of Direct Blue-86 dye from aqueous solution using alginate encapsulated activated carbon (PnsAC-alginate) prepared from waste peanut shell. *J. Environ. Chem. Eng.*, 7, 103365. <https://doi.org/10.1016/j.jece.2019.103365>
9. Gökırmak Söğüt, E. 2022. Effect of chemical and thermal treatment priority on physicochemical properties and removal of crystal violet dye from aqueous solution. *ChemistrySelect*, 7, e202200262. <https://doi.org/10.1002/slct.202200262>
10. Kali, A., Amar, A., Loulidi, I., Jabri, M., Hadey, C., Lgaz, H., Alrashdi, A.A., Boukhlifi, F. 2022. Characterization and adsorption capacity of four low-cost adsorbents based on coconut, almond, walnut, and peanut shells for copper removal. *Biomass Convers. Biorefinery*. <https://doi.org/10.1007/s13399-022-02564-4>
11. Khan, A.A., Gul, J., Naqvi, S.R., Ali, I., Farooq, W., Liaqat, R., AlMohamadi, H., Štěpanec, L., Juchelková, D. 2022. Recent progress in microalgae-derived biochar for the treatment of textile industry wastewater. *Chemosphere*, 306, 135565. <https://doi.org/10.1016/j.chemosphere.2022.135565>
12. Khaniabadi, Y.O., Mohammadi, M.J., Shegerd, M., Sadeghi, S., Saeedi, S., Basiri, H. 2017. Removal of Congo red dye from aqueous solutions by a low-cost adsorbent: activated carbon prepared from Aloe vera leaves shell. *Environ. Health Eng. Manag.*, 4(1), 29–35. <https://doi.org/10.15171/EHEM.2017.05>
13. Khatami, S., Deng, Y., Tien, M., Hatcher, P.G. 2019. Lignin contribution to aliphatic constituents of humic acids through fungal degradation. *J. Environ. Qual.*, 48, 1565–1570. <https://doi.org/10.2134/jeq2019.01.0034>
14. Khiaophong, W., Jaroensan, J., Kachangoon, R., Vichapong, J., Burakham, R., Santaladchaiyakit, Y., Srijaranai, S. 2022. Modified peanut shell as an eco-friendly biosorbent for effective extraction of triazole fungicide residues in surface water and

- honey samples before their determination by high-performance liquid chromatography. *ACS Omega*, 7(39), 34877–34887. <https://doi.org/10.1021/acsomega.2c03410>
15. Lucaci, A.R., Bulgariu, D., Ahmad, I., Bulgariu, L. 2020. Equilibrium and kinetics studies of metal ions biosorption on alginate extracted from marine red algae biomass (*Callithamnion corymbosum* sp.). *Polymers*, 12(9), 1888. <https://doi.org/10.3390/polym12091888>
 16. Marszałek, J., Żyła, R. 2021. Recovery of water from textile dyeing using membrane filtration processes. *Processes*, 9(10), 1833. <https://doi.org/10.3390/pr9101833>
 17. Orooji, Y., Han, N., Nezafat, Z., Shafiei, N., Shen, Z., Nasrollahzadeh, M., Karimi-Maleh, H., Luque, R., Bokhari, A., Klemeš, J.J. 2022. Valorisation of nuts biowaste: Prospects in sustainable bio (nano) catalysts and environmental applications. *J. Clean Prod.*, 347, 131220. <https://doi.org/10.1016/j.jclepro.2022.131220>
 18. Pavan, F.A., Lima, E.C., Dias, S.L., Mazzocato, A.C. 2008. Methylene blue biosorption from aqueous solutions by yellow passion fruit waste. *J. Hazard. Mater.*, 150, 703–712. <https://doi.org/10.1016/j.jhazmat.2007.05.023>
 19. Peng, H., Guo, J. 2020. Removal of chromium from wastewater by membrane filtration, chemical precipitation, ion exchange, adsorption electrocoagulation, electrochemical reduction, electro dialysis, electrodeionization, photocatalysis and nanotechnology: a review. *Environ. Chem. Lett.*, 18, 2055–2068. <https://doi.org/10.1007/s10311-020-01058-x>
 20. Rashid, R., Shafiq, I., Akhter, P., Iqbal, M.J., Hussain, M. 2021. A state-of-the-art review on wastewater treatment techniques: the effectiveness of adsorption method. *Environ. Sci. Pollut. Res.*, 28, 9050–9066. <https://doi.org/10.1007/s11356-021-12395-x>
 21. Saghir, S., Pu, C., Fu, E., Wang, Y., Xiao, Z. 2022. Synthesis of high surface area porous biochar obtained from pistachio shells for the efficient adsorption of organic dyes from polluted water. *Surfaces and Interfaces*, 34, 102357. <https://doi.org/10.1016/j.surfin.2022.102357>
 22. Sah, M.K., Edbey, K., EL-Hashani, A., Almsheety, S., Mauro, L., Alomar, T.S., AlMasoud, N., Bhattarai, A. 2022. Exploring the biosorption of methylene blue dye onto agricultural products: A critical review. *Separations*, 9(9), 256. <https://doi.org/10.3390/separations9090256>
 23. Sahmoune, M.N. 2019. Evaluation of thermodynamic parameters for adsorption of heavy metals by green adsorbents. *Environ. Chem. Lett.*, 17, 697–704. <https://doi.org/10.1007/s10311-018-00819-z>
 24. Sarojini, G., Babu, S.V., Rajamohan, N., Rajasimman, M. 2022. Performance evaluation of polymer-marine biomass based bionanocomposite for the adsorptive removal of malachite green from synthetic wastewater. *Environ. Res.*, 204, 112132. <https://doi.org/10.1016/j.envres.2021.112132>
 25. Sawalha, H., Bader, A., Sarsour, J., Al-Jabari, M., Rene, E.R. 2022. Removal of dye (methylene blue) from wastewater using bio-char derived from agricultural residues in Palestine: Performance and isotherm analysis. *Processes*, 10(10), 2039. <https://doi.org/10.3390/pr10102039>
 26. Senthil Kumar, P., Abhinaya, R.V., Gayathri Lashmi, K., Arthi, V., Pavithra, R., Sathyaselvabala, V., Dinesh Kirupha, S., Sivanesan, S. 2011. Adsorption of methylene blue dye from aqueous solution by agricultural waste: Equilibrium, thermodynamics, kinetics, mechanism and process design. *Colloid J.*, 73, 651–661. <https://doi.org/10.1134/S1061933X11050061>
 27. Teshager, F.M., Habtu, N.G., Mequanint, K. 2022. A systematic study of cellulose-reactive anionic dye removal using a sustainable bioadsorbent. *Chemosphere*, 303, 135024. <https://doi.org/10.1016/j.chemosphere.2022.135024>
 28. Turan, A.Z., Turan, M. 2022. Removal of heavy metals and dyes from wastewaters by raw and activated carbon hazelnut shells. In: *Progress in Nanoscale and Low-Dimensional Materials and Devices*. Springer Topics in Applied Physics. Springer, Cham., 144, 907–933. https://doi.org/10.1007/978-3-030-93460-6_31
 29. Uddin, M.K., Nasar, A. 2020. Walnut shell powder as a low-cost adsorbent for methylene blue dye: isotherm, kinetics, thermodynamic, desorption and response surface methodology examinations. *Sci. Rep.*, 10, 1–13. <https://doi.org/10.1038/s41598-020-64745-3>
 30. Vishnu, D., Dhandapani, B., Authilingam, S., Sivakumar, S.V. 2022. A comprehensive review of effective adsorbents used for the removal of dyes from wastewater. *Curr. Anal. Chem.*, 18, 255–268. <https://doi.org/10.2174/1573411016999200831111155>
 31. Yu, H., Wang, T., Yu, L., Dai, W., Ma, N., Hu, X., Wang, Y. 2016. Remarkable adsorption capacity of Ni-doped magnolia-leaf-derived bioadsorbent for congo red. *J. Taiwan Inst. Chem. Eng.*, 64, 279–284. <https://doi.org/10.1016/j.jtice.2016.04.008>